JACS
JOURNAL OF THE AMERICAN CHEMICAL SOCIETY
Article
pubs.acs.org/JACS

Iodine Release and Recovery, Influence of Polyiodide Anions on Electrical Conductivity and Nonlinear Optical Activity in an Interdigitated and Interpenetrated Bipillared-Bilayer Metal–Organic Framework

Zheng Yin, Qiang-Xin Wang, and Ming-Hua Zeng*

Key Laboratory for the Chemistry and Molecular Engineering of Medicinal Resources (Ministry of Education), School of Chemistry & Chemical Engineering, Guangxi Normal University, Guilin 541004, People's Republic of China

Supporting Information

ABSTRACT: $\{[Cu_6(pybz)_8(OH)_2]\cdot I_5^-\cdot I_7^-\}_n$ (**1**), obtained hydrothermally by using iodine molecules as a versatile precursor template, consists of a cationic framework with two types of zigzag channels, which segregate I_5^- and I_7^- anions. The framework exhibits the first observed bipillared-bilayer structure featuring both interdigitation and interpenetration. **1** displays high framework stability in both acidic (HCl) and alkaline (NaOH) solutions. **1** slowly releases iodine in dry methanol to give $[Cu_6(pybz)_8(OH)_2](I^-)_2\cdot 3.5CH_3OH$ (**1′**) and partially recovers iodine from cyclohexane to form $[Cu_6(pybz)_8(OH)_2](I^-)_2\cdot xI_2$ (**1″**). Differences of up to 100 times in electrical conductivity and of 4 times in nonlinear optical activity (NLO) have been measured between **1** and **1′**. This compound is one of few displaying multifunctionality, electrical conductivity, NLO, and crystal–crystal stability upon release and recovery of iodine. It is also unique in the iodine release from polyiodide anions in a metal–organic framework.

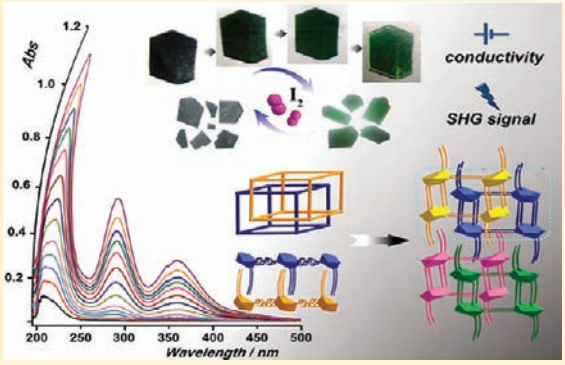

1. INTRODUCTION

During the past few years, the research on microporous metal–organic frameworks (MMOFs) has been very fruitful,[1] driven by the desire to acquire molecule-based porous materials having different functions and to understand their structure–property relationships.[2] One important synthetic strategy to create MMOFs is the introduction of appropriate organic guests as template trapped within the framework that can be released easily.[3] Also then, through removal/inclusion of different guest molecules, the acquired MMOFs are good candidates to study the storage/sorption capacities and other physicochemical properties.[4] MMOFs with iodine as guest are still limited,[5,6] but are especially fascinating because of the particular chemistry of iodine such as polarity,[7] oxidizability,[8] and conductivity.[9] On the other hand, the enrichment of radioactive iodine, a major waste of the nuclear industries, using special MMOFs as effective porous adsorbents is beneficial for clean nuclear energy.[6a] In fact, in most reported MMOFs bearing iodine guests, the iodine molecules were introduced by guest exchange in iodine solution[5,8] or by diffusion in high concentration iodine vapor.[6,9] In our previous work,[10] we chose 4-pyridyl benzoate (pybz) and DL-lactate to create double-walled MMOFs $\{[Zn_3(DL\text{-}lac)_2(pybz)_2]\cdot 3DMF\}_n$ (lacZn·3DMF) using DMF as the organic template. After introduction of iodine molecules as new guests by two-step crystalline state transformation, a marked electrical conductivity increase resulted from the host–guest interaction, cooperatively increasing the polar effect.

However, the inherent difficulties for the above study can be summarized as: (i) the introduction of sufficient iodine guest is never easy; and (ii) the final MMOFs with iodine guest are often poorly crystalline, hence hampering structural characterizations, especially determining the exact position of iodine.[5−10] Given the possible multiple species of iodine such as I_2, I_{2n+1}^- in aqueous solution,[11] and their limited solubility,[12] the direct addition of iodine as precursor template at the beginning of the synthesis may acquire MMOFs with iodine molecules or different forms of polyiodide anions trapped in the lattice during the slow release and then self-assembly processing.[13]

Inspired by the above principles and our previous work, here we report a polyiodide anions inclusion MMOF $\{[Cu_6(pybz)_8(OH)_2]\cdot I_5^-\cdot I_7^-\}_n$ (**1**), which was synthesized under hydrothermal condition by introducing iodine molecule as a versatile precursor template (Scheme 1). This compound exhibits unique structural features combining interdigitation and interpenetration based on a bipillared-bilayer framework. Furthermore, we explored its kinetics of iodine molecule release and recovery through crystal transformation, and, for the first time, probed the modulated effect of polyiodide anions on the

Received: December 5, 2011
Published: February 21, 2012

   dx.doi.org/10.1021/ja211381e | J. Am. Chem. Soc. 2012, 134, 4857–4863

Scheme 1. Schematic Presentation of the Preparation of 1 Using Iodine as the Precursor Template

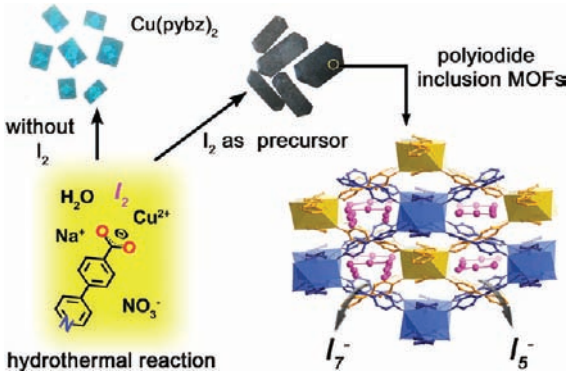

electrical conductivity and nonlinear optical activity between the as-synthesized sample and neutral iodine released sample.

2. EXPERIMENTAL SECTION

2.1. Synthesis of the Compounds. A mixture of 4-pyridylbenzoate (0.224 g, 1 mmol), $Cu(NO_3)_2{\cdot}3H_2O$ (0.162 g, 0.67 mmol), iodine (0.160 g, 0.63 mmol), and H_2O (15.0 mL) was stirred for 10 min in air. Next, the mixture was placed in a 23 mL Teflon-lined autoclave and heated at 140 °C for 72 h. The autoclave was cooled over a period of 12 h at a rate of 10 °C h^{-1}, and black block crystals $\{[Cu_6(pybz)_8(OH)_2]{\cdot}I_5^-{\cdot}I_7^-\}_n$ (**1**) were collected by filtration, washed with water, and dried at ambient temperature. Yield: 32% (based on Cu). The phase purity of the bulk product was confirmed by powder X-ray diffraction (XRD). Anal Calcd for **1**: C, 32.72; H, 1.89; N, 3.18. Found: C, 32.43; H, 2.02; N, 3.16. IR: 3420 (w), 1595 (vs), 1563 (s), 1379 (vs), 1403 (s), 1222 (m), 1187 (m), 1073 (w), 1042 (w), 1010 (w), 829 (m), 776 (s), 762 (m).

Upon immersion of the black crystals of **1** in dry methanol for 30 days in a 25 mL glass bottle with three times renewal of the methanol repeatedly every day, the neutral iodine guest molecules were exchanged by MeOH, and green crystals of $[Cu_6(pybz)_8(OH)_2]$-$(I^-)_2{\cdot}3.5CH_3OH$ (**1′**) were then obtained. TGA and elemental analysis confirm the complete exchange of neutral iodine guest as well as the number of CH_3OH per molecular unit. Anal. Calcd for **1′**: C, 50.58; H, 3.34; N, 4.76. Found: C, 50.41; H, 3.16; N, 4.85. IR: 3426 (m, b), 2059 (w), 1593 (vs), 1562 (vs), 1393 (vs), 1221 (m), 1181 (m), 1075 (m), 1009 (m), 831 (m), 779 (s), 490 (m).

2.2. X-ray Crystallography. The single-crystal diffraction data were collected on a Bruker Smart Apex CCD diffractometer using graphite monochromated Mo Kα radiation (λ = 0.71073 Å). Absorption corrections were applied by using multiscan program SADABS.[14] The structure was solved by direct methods and refined by the full-matrix least-squares method on F^2 using the SHELXTL program package.[15] All non-hydrogen atoms were refined with anisotropic displacement parameters. The hydrogen atoms on the μ_3-OH bridge were located from difference maps. Hydrogen atoms on the organic ligands were generated by the riding model (C–H 0.95 Å). Crystal data as well as details of data collection and refinements are summarized in Table 1. Selected bond distances and bond angles are listed in Table S1. The supplementary crystallographic data for this compound can be found in the Supporting Information or can be obtained free of charge from the Cambridge Crystallographic Data Centre quoting CCDC-856471 via http://www.ccdc.cam.ac.uk/data_request/cif.

2.3. Measurement Details. The reagents and solvents employed were commercially available and used as received without further purification. The C, H, and N microanalyses were carried out with a Perkin-Elmer PE 2400 II CHN elemental analyzer. The FT-IR spectra were recorded from KBr pellets in the range of 4000–400 cm^{-1} on a Perkin-Elmer FTIR spectrophotometer. Thermogravimetry analyses were performed on a Netzsch TG 209 instrument. Powder X-ray diffraction (PXRD) measurements were performed on a Bruker D8 ADVANCE X-ray diffractometer with Cu Kα radiation. The crystalline powder samples were prepared by crushing the single crystals and scanned from 3° to 60° with a step of 5°/min. Calculated patterns of **1** were generated with PowderCell. Raman spectra were obtained using a Renishaw inVia Raman microscope equipped with a 785 nm diode laser and a 1200 lines/mm grating. UV/vis spectrophotometer was recorded within the wavelength range 190–600 nm using the same solvent in the examined solution as a blank. The sorption isotherms for carbon dioxide were measured using an ASAP 2020 adsorption system. The as-synthesized samples were treated by heating at 100 °C for 10 h in a quartz tube under a vacuum to remove the solvent molecules. Electrical measurements (Keithley Source meter 2400) on crystals powders were performed on a 0.2 mm thick sample piece by DC four electrodes methods. The powder SHG test was carried out on the sample by the Kurtz–Perry method. The sample was powdered to approximate spherical shape and graded by standard sieves to 8–105 μm. The samples were then placed in a 0.2 mm thick quartz cell and irradiated by a Q-switched Nd: YAG solid-state laser (1064 nm, 10 kHz, 10 ns). We measured the intensity of the frequency-doubled output emitted from the sample using a photomultiplier tube. The second harmonic efficiency of the sample was compared to that of a standard powder sample of KDP (KH_2PO_4).

Table 1. Crystallographic Data for 1

	1
formula	$Cu_6C_{96}H_{66}N_8O_{18}I_{12}$
formula weight	3551.68
temperature/K	150(2)
crystal system	orthorhombic
space group	*Pcc*2
a/Å	27.686 (1)
b/Å	27.767 (1)
c/Å	13.993 (1)
V /Å^3	10757.6 (9)
Z	4
D_c/g cm^{-3}	2.193
Flack parameter	0.001(1)
F(000)	6664
reflns collected	42 841
unique reflns	17 846
R_{int}	0.022
$R_1{}^a$ values [$I > 2\sigma(I)$]	0.0887
$wR_2{}^b$ (all data)	0.2565
GOF	1.06

$^aR_1 = \sum||F_o| - |F_c||/\sum|F_o|$. $^bwR_2 = [\sum w(F_o^2 - F_c^2)^2/\sum w(F_o^2)^2]^{1/2}$.

3. RESULTS AND DISCUSSION

Compound **1** crystallizes in the tetragonal *Pcc*2 space group, and the asymmetric unit consists of 6 independent Cu^{2+} ions, 8 pybz ligands, and 12 iodine atoms (Figure 1a). The 6 Cu^{2+} ions form two similar μ_3-OH-bridged tricopper units (Figure 1b).

Among the copper atoms, two are five-coordinated Cu^{2+} and one is four-coordinated Cu^{2+}, which are encapsulated by four carboxylate groups and three pyridyl groups of pybz (Figure 1b). The Cu–O, Cu–N distances are in the range of 1.918(1)–2.110(1) and 1.959(1)–2.003(4) Å, respectively.

The trimers are extended through four pybz ligands in a tridentate μ_3:η_1:η_1:η_1 form in the *bc* plane into an infinite (4, 4) sheet with a rhombic window size of ca. 15.6 × 15.6 Å^2 (center to center of adjacent trimers). Two such sheets are further linked by pairs of pybz ligands into a bipillared-bilayer with an interlayer distance of ca. 14.5 Å (Figure 2). Interestingly, the remaining pybz serve as dangling arms on the sheet with a

dx.doi.org/10.1021/ja211381e | J. Am. Chem. Soc. 2012, 134, 4857–4863

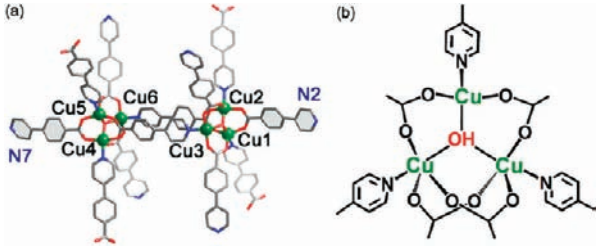

Figure 1. (a) The coordination environment of Cu^{2+} ions in **1**; N2 and N7 were coordination suspended. General color code: Cu, green; N, blue; O, red; C, gray-50% (H atoms are not shown for clarity). (b) Perspective view of the μ_3-OH-bridged tricopper unit.

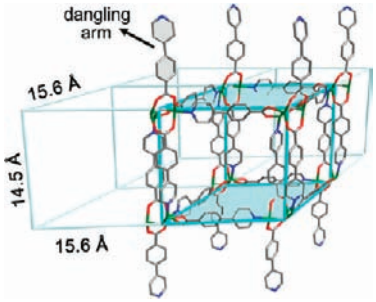

Figure 2. Perspective view of the bipillared-bilayer with cuboidal boxes and dangling pybz arms.

μ_2:η_1:η_1 coordination mode, using the carboxylate groups to bridge pairs of Cu^{2+} ions in the trimer, while the nitrogen atom remains uncoordinated. From another point of view, the bipillared-bilayer consists of face-sharing cuboidal boxes (ca. 15.6 × 15.6 × 14.5 $Å^3$) with the slender pybz ligands as the edges.

As is well-known, interpenetration easily occurs under the above condition.[16] A pair of bilayers interpenetrate each other in a parallel/parallel inclined fashion with the double pybz pillars inserting the rhombic windows while the cuboidal box encloses the tricopper node,[16,17] resulting in 2D+2D→2D architecture (Figures 3, S2). Further, the slender dangling pybz

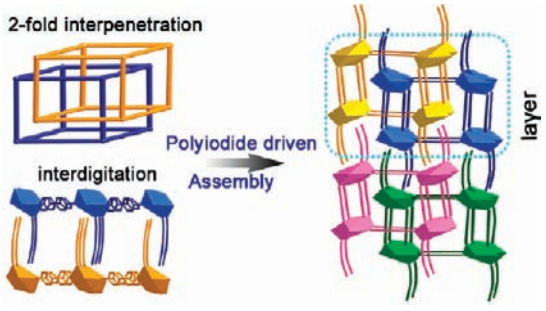

Figure 3. Proposed structural evolution from 2-fold interpenetration and interdigitation into 3D motif in AAA packing fashion, in which the tricopper unit was simplified to a polyhedron.

ligands point into the voids of adjacent interpenetrated pillar-bilayers, resulting in a novel 2D to 3D interdigitated array in **1** (Figure 3). Strong hydrogen bonding (O−H···N = 2.629−2.654 Å) and weak offset $\pi-\pi$ interaction (3.578−3.601 Å) were found to further stabilize the 3D supramolecular structure (Figure S3).[18]

Interestingly, the 3D structure of **1** represents a rare example of 2D bipillar-bilayer motif with bifunctional pybz ligands serving simultaneously as single bridges in the sheets and as bipillars in the bilayer.[19] To our best knowledge, the evolution from pillar-bilayer to 2D+2D→2D interpenetration, then interdigitated architecture through the dangling arms, is unprecedented.[20] Although the formation of **1** is serendipitous, this finding provides valuable insights into the self-catenation or polyknotting networks.[16,21]

More interestingly, even in the presence of mutual interpenetration and interdigitation, there are two kinds of zigzag 1D channels (A and B) running along the *a* axis in **1** (Figure 4a). Channels A and B with a largest dimension of ca.

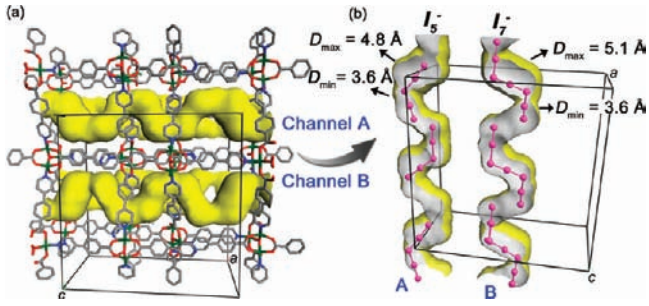

Figure 4. (a) Perspective of the S-shape 1D channels along the *a* axis. (b) Section drawing of the A and B channels in each cell lattice.

4.8 and 5.1 Å possess corresponding void volumes of 15.9% and 21.7%, using PLATON,[22] occupied by I_5^- and I_7^- ions in A and B channels, respectively (Figure 4b). In fact, the effective free volume (V_{void}) of 26.9% was calculated by removing all of the neutral iodine guests. It should be noted that the iodine content is high to about 43.2% (wt %), which is competitive with the traditional methods of introducing iodine (Table S2). The I_5^- and I_7^- ions are derived from I^- ions with two or three I_2 molecules. The I_2 units [I−I distance, ca. 2.755−2.856 Å] and I^- anion have distances in the range of ca. 2.915−3.239 Å.[23] However, the closest distance between adjacent I_5^- or I_7^- units in the channel of 4.226 and 3.973 Å, respectively, hampers the formation of longer polyiodide anions. It should be noted that both the I_5^- and the I_7^- were tightly surrounded by the aromatic rings of channel walls, and most of the I···C distances are in a range less than 4.0 Å with the closest distance of only 3.685 Å (Figures 5, S4).

Obviously, it is a great challenge to demonstrate the assembly procedure of **1**.[1] However, to observe the possible change of precursor iodine template during the reaction may be simple,

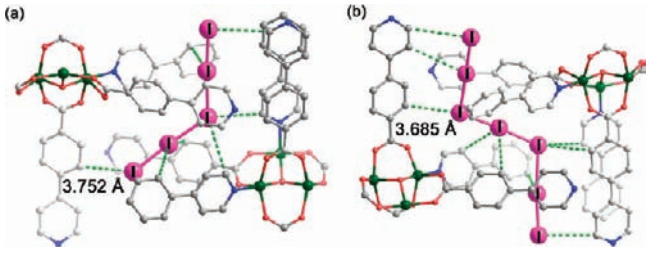

Figure 5. (a) The environment of I_5^- in channel A; the distances from I atoms to C atoms of phenyl or pyridyl rings are in the range of 3.732−3.999 Å. (b) The environment of I_7^- in channel B; the distances from I atoms to C atoms of phenyl or pyridyl rings are in the range of 3.685−4.281 Å.

dx.doi.org/10.1021/ja211381e | J. Am. Chem. Soc. 2012, 134, 4857−4863

and it is also important to know some probable forming process of such a special compound.[24] Photos of the reaction mixture in the course of synthesis of **1** reveal the color became darker gradually while the crystal size and yield increased as the reaction time was prolonged (Figures S5, S6). UV/vis absorption spectra of the filtrate of the reaction mixture collected at different times confirm the polyiodide ions in low concentration can be found at an early stage (4 h), and the concentration of polyiodide ions increased remarkably along with prolonged reaction time (Figure S7). On the other hand, in a contrast synthesis without iodine as reactant, blue octahedral crystals were obtained (Figure S5), which is a known compound $[Cu(pybz)_2]_n$, as confirmed by PXRD patterns (Figure S8), having a dense, interlocking framework with two independent 3D networks based on single copper nodes.[25] Taking the above information into consideration, we can infer that the iodine molecules act as slow released precursor and were transformed to polyiodide ions in the hydrothermal condition, which then participated in and drove the formation of the 3D supramolecular network of **1**.

The thermal stability of **1** was investigated by TG and temperature-dependent PXRD. The TG curve of **1** shows remarkable weight loss without obvious platform over 25−800 °C (Figure S9). The PXRD patterns appear to have similar shape and intensity below 200 °C; only very slight shifts of some peaks to lower θ angle were noted, which may be attributed to the change of torsional angles of the ligand coupling with a release of the iodine molecules under heating (Figure S10).[19a,26] After heating the crystals of **1** in boiling water for 3 days, no significant change of either the external appearance or the PXRD patterns was found for the sample. Moreover, under ambient condition, the unchanged PXRD patterns also confirm extreme framework stability of **1** after long time storage in air even up to 1 year (Figures S10−12).

More interestingly, after placing **1** in hydrochloric acid solution (pH = 3) or sodium hydroxide solution (pH = 12) for 24 h, the Raman spectroscopy patterns maintain similar peak shape and position (Figure 6). The almost unchanged prominent singlet bands at 1615 and 1292 cm^{-1} were assigned to aromatic-ring stretching vibration and in-plane symmetric C−H stretching vibration of pybz ligand.[27] Also, the wide band at 328 cm^{-1} due to coordination bonding vibration did not shift as well, only with the peak intensity did it weaken slightly.[27] So

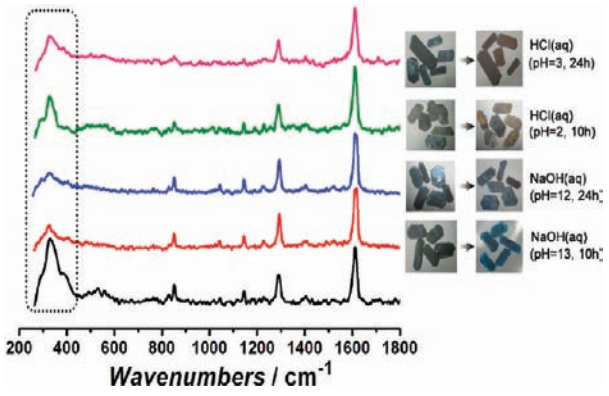

Figure 6. Raman spectra of **1** after soaking in different acid or base solutions. The photos of the crystals before and after soaking in acid or base solutions are shown in the right side of each spectrum, respectively.

the crystals of **1** show certain resistance to acid/base aqueous solution, and such high acid/base stability has not been documented in MMOFs with iodine or polyiodide guests and is also very rare in reported MOFs. Obviously, the close packing and very strong supramolecular interactions between the electropositive framework and polyiodide ions and their hydrophobic nature are crucial for the improved stability of **1**.[1,28]

Inspired by the stable host framework of **1** and the controlled uptake and release of iodine molecules in our previous work,[10] we tried to realize iodine release and recovery through guest exchange reaction in an opposite direction. When crystals of **1** were soaked in dry methanol, the color of the methanol solution changed gradually from colorless to pale yellow, and then deepens to a darker yellow (Figure 7a). After renewal of

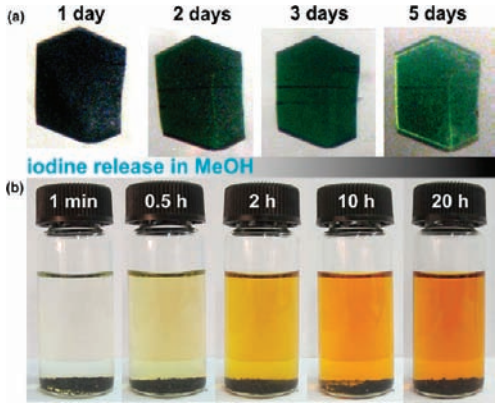

Figure 7. (a) Color transformation from black to green of a thin single crystal of **1**. (b) Iodine releasing process of **1** (30 mg) soaked in 3.5 mL of MeOH.

the methanol repeatedly many times, the colors of the crystals of **1** change from black to green (Figure 7b). The final methanol exchanged phase $[Cu_6(pybz)_8(OH)_2]\cdot(I^-)_2\cdot 3.5CH_3OH$ (**1′**) was obtained. Its composition was confirmed by TG and elemental analyses (Figure S13). Temperature-dependent PXRD patterns of **1′** indicated that the framework is maintained after the removal of guest methanol molecules in the temperature range of 30−100 °C. However, upon further heating, shifts of some peaks to lower θ angle were observed, implying the possible distortion (100−230 °C) of pybz linkers, even deformation and decomposition (above 260 °C) of the host framework (Figure S14).

Accurate comparison of the constituents in the channels of **1** and **1′**, where the new guest MeOH has replaced the separating I_2, reminds us that a new kind of crystalline transformation has taken place featuring unusual decomposition reaction of polyiodide anions: $I_5^- \rightarrow 2I_2 + I^-$ and $I_7^- \rightarrow 3I_2 + I^-$.[29] So we did much work to investigate this transformation. First, we selected proper single crystals with very similar shape and size, and soaked them in dry MeOH (50 mL) in a volumetric flask, followed by replacement of MeOH many times.

The cell parameters measured for the partial iodine released single crystals at different time show slight increases (1−2%) as compared to the virgin crystal and the same space group (Figure 8a, Table S3). Moreover, under heating in N_2 flow at different temperatures, the crystal system and space group of the iodine partially released single crystals were also maintained with slight cell volume increase of 0.5−1.5% (Figure 8b, Table S4). However, when we tried to find a size of single crystal of **1′**

dx.doi.org/10.1021/ja211381e | J. Am. Chem. Soc. 2012, 134, 4857−4863

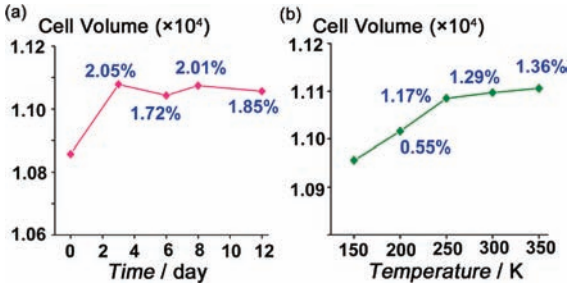

Figure 8. (a) Cell parameters measurement (150 K) of partly iodine released single crystal at different time. (b) Cell parameters measurement for the iodine released single crystal soaked in MeOH for 12 days at different temperatures.

for X-ray crystal structure analysis, several crevices were found on the crystals after long time I_2 release process. Next, a small piece of single crystal obtained by careful cutting was used for crystallographic studies using an Oxford Gemini AUltra diffractometer with graphite monochromated Cu Kα radiation (λ = 1.5418 Å). In the pre-experiment, the existence of good diffraction image point at low angle (Figure S15a) (exposure time = 30 s, resolution > 3.3 Å) confirms the single crystalline state was maintained to a certain degree. However, the absence of clear diffraction spots at high angle (exposure time = 120 s, resolution < 1.1 Å) suggested the weak diffraction ability of **1′** (Figure S15b). After all data collection, a reasonable structural model was not obtained, which resulted from the very poor resolution factor of the crystallographic data. Yet the aforementioned crystallographic studies indicated **1′** did not cause the obvious change of the host framework and the channels, during the gradual decomposition of the polyiodide I_5^- and I_7^- to I^- and I_2, along with the exchange of I_2 by MeOH through the crystal transformation processing.

To further investigate the kinetics of I_2 delivery of **1** in crystal transformation, in situ UV/vis spectrum was recorded at room temperature (Figure 9). The absorbance of I_2 in methanol

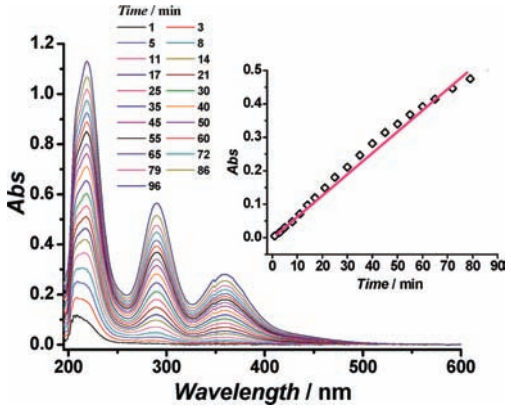

Figure 9. Temporal evolution of UV/vis absorption spectra for the I_2 delivery from a single crystal of **1** in 3 mL of MeOH. Inset: The controlled delivery of I_2 ($[I_2] = Kt$) in the first 1.5 h (down).

increases linearly with time, which is empirically adjusted as a zero-order equation. The releasing rate of iodine in **1** was estimated to be about 80 I_2/s from each window of the channels based on the results that a regular single crystal with 0.6 × 0.5 × 0.5 mm^3 size released 6.1 × 10^{-5} g of I_2 in a colorimetric cell with 3 mL of methanol in the first 1.5 h (Figure S16). The iodine release rate becomes slower later because the concentration of I_2 in methanol increases with time. The complete release of iodine needs more than 20 days with renewal of methanol continuously. The initial releasing rate of **1** in the first 1.5 h is lower than that of lacZn·3I_2 (170 I_2/s per window).[10] In lacZn·3I_2, the regular nanospace combining with abundant π-electron walls and well-defined host−guest interaction cumulate the advantages of controlled uptake and release of I_2. However, in **1**, the progressive decomposition of poly iodide I_5^- and I_7^- to I^- and I_2, the effective host−guest interaction, in addition with the smaller and irregular channels cooperatively intensify the controlled release of I_2 and resulted in a lower release rate.

Of further interest, by removing methanol guest of **1′** by heating and then soaking the nonsolvated phase in a saturated cyclohexane solution of iodine, a partial iodine recovered phase $[Cu_6(pybz)_8(OH)_2](I^-)_2{\cdot}xI_2$ (**1″**) was obtained (Figure 10).

Figure 10. (a) Photos of the color change of guest removed crystals of **1′** to iodine recovered **1″**. (b) Photos of the iodine recovery process with 400 mg of desolvated crystals of **1′** soaked in cyclohexane solution of I_2 (0.1 M/L, 3.5 mL).

The maximum value of x was in the range of 2.2−2.6 depending on individual experiments (Figure S17). For lacZn·3I_2, the complete recovery of I_2 was attributed to the exceptional affinity of the linear, rigid, regular channel, and π-electron walls for I_2. The reduced amount of iodine recovered by **1′** is not only influenced by flexibility of the channels and the irregular π-electron walls, but also by the difficulty of reforming the polyiodide anions.

The sorption behaviors of methanol removed phase of **1′** were investigated using CO_2 as a probe molecule. It adsorbs CO_2 of 27.6 (293 K) and 55.1 (195 K) cm^3 (STP) g^{-1} at 760 Torr (Figure S18), respectively. However, it does not exhibit the classically reversible type-I isotherms, but instead a noticeable hysteresis for CO_2 desorption. The hysteresis can be attributed to the hindered escape due to the residual iodine ions in the channels. From the CO_2 sorption isotherm at 195 K, a BET surface area of 131.6 m^2 g^{-1} is estimated, which further confirms the permanent porosity. This value is understandably uncompetitive as compared to the high surface areas of 3D MMOFs, but it was comparable to some reported interdigitated structures.[18,30] Moreover, the characteristic peaks of PXRD patterns of **1′** keep their intensities and positions after the

dx.doi.org/10.1021/ja211381e | J. Am. Chem. Soc. 2012, 134, 4857−4863

sorption experiment, which further confirms the stability of the porosity (Figure S19).

As the iodine location in **1** was determined by single-crystal diffraction and the neutral iodine removal phase (**1′**) can be easily obtained through crystal transformation, it provided us a precious chance to compare the influence of polyiodide anions on host–guest cooperative properties. Electrical conductivity values (σ) of 8.11×10^{-7} S/cm for **1** (10 times the generally accepted value of 7.69×10^{-8} S/cm for solid I_2) and 8.04×10^{-9} S/cm for **1′** (about one tenth of that of solid I_2) were obtained for measurements on film samples of crushed crystals at room temperature. For comparison, the anisotropic conductivities of lacZn_3I_2 were found to be ca. 3.42×10^{-3} ($\sigma_{\parallel}$) and 1.65×10^{-4} ($\sigma_{\perp}$) S/cm, respectively. These significantly greater values than that of solid I_2 can be ascribed to that the four close parallel iodine chains are restricted within well-regulated aromatic nanochannels, inducing high efficiency of n → σ^* charge-transfer (CT).[2c,10] On the other hand, the lower conductivity of **1** can be partly attributed to the loose packing of I_5^- or I_7^- in **1** as indicated by the distance between adjacent polyiodide ions. Moreover, the positively charged framework and irregular π-electron walls may be disadvantageous for the effective charge transfer. However, the structural evidence of linear polyiodide ions array, supramolecular interactions between I_2 and π-electron walls, in addition to the measurable conductivity difference between **1** and **1′** demonstrate in detail that well-regulated array of iodine or polyiodide ions surrounded by π-electron walls can contribute to increasing cooperative electrical conductivity in MMOFs.

Moreover, beyond our expectation, we found that the *Pcc*2 space group within the point group C_{2v} is quite unusual. There are only 10 reported compounds including five organic compounds crystallizing in this space group in the CCDC database (Table S5). In fact, **1** was the first 3D-metal based MOF crystallizing in the *Pcc*2 space group.[31] As this space group is noncentrosymmetric, the powder second harmonic generation (SHG) test was carried out for **1** and **1′** using the Kurtz–Perry method.[32] The resulting SHG signals were about 2.0 and 0.5 times that of KDP, respectively. These SHG signals are of considerable level to most reported second-order nonlinear optical active coordination polymers.[33] The 4 times difference in SHG signals indicates that the more effective polarization contribution is from the I_5^- and I_7^- rather than I^- and probably also as a consequence of the regular array of polyiodide, resulting in a dipole moments aligned in same directions. The example suggests a new approach for the modulation of nonlinear optical activity for MMOFs by the presence and absence of polyiodide anions.

4. CONCLUSION

In summary, a polyiodide anion-driven assembly of a bipillared-bilayer MMOF is reported, which unexpectedly achieves marriage of interdigitation with 2-fold interpenetration. It also shows a rare and vivid example of iodine release, partial iodine recovery, and electrical conductivity and nonlinear optical activity modulated by crystalline transformation associated with decomposition of polyiodide ions. The results highlight the prominent influence of functional guests encapsulated in pores on the host–guest cooperative properties in MMOFs. Furthermore, rational synthesis using target guest, such as iodine, opens a promising approach for constructing functional guest encapsulated MMOFs with new structural topology and interesting properties.

■ ASSOCIATED CONTENT

Supporting Information

Addition files, synthesis, crystal data in CIF files, IR, TG, PXRD, and UV/vis spectrum data. This material is available free of charge via the Internet at http://pubs.acs.org.

■ AUTHOR INFORMATION

Corresponding Author

zmh@mailbox.gxnu.edu.cn

Notes

The authors declare no competing financial interest.

■ ACKNOWLEDGMENTS

This work was supported by NSFC (nos. 91022015, 91122032), the Program for New Century Excellent Talents in University of the Ministry of Education China (NCET-07-217), the Project of Ten, Hundred, Thousand Distinguished Talents in New Century of Guangxi (no. 2006201), and GXNSFC (2010GXNSFF013001), as well as the Project of Talents Highland of Guangxi Province, and the Project of Talents Highland of Colleges and Universities in Guangxi Province. We thank Prof. La-Sheng Long at Xiamen University for electrical measurements. We also thank Dr. Li Wang at the Xinjiang Technical Institute of Physics & Chemistry (CAS) for nonlinear optical activity measurements.

■ REFERENCES

(1) (a) Batten, S. R.; Neville, S. M.; Turner, D. R. Coordination. *Polymers Design, Analysis and Application*; The Royal Society of Chemistry: London, 2009; pp 273–372. (b) Farrusseng, D. *Metal–Organic Frameworks: Applications from Catalysis to Gas Storage*; John Wiley and Sons: New York, 2011; pp 1–103.

(2) (a) Horike, S.; Shimomura, S.; Kitagawa, S. *Nat. Chem.* **2009**, *1*, 695–704. (b) Kreno, L. E.; Leong, K.; Farha, O. K.; Allendorf, M.; Duyne, R. P. V.; Hupp, J. T. *Chem. Rev.* **2012**, *112*, 1105–1125. (c) Meek, S. T.; Greathouse, J. A.; Allendorf, M. D. *Adv. Mater.* **2011**, *23*, 249–267. (d) Zhang, J.-P.; Zhang, Y.-B.; Lin, J.-B.; Chen, X.-M. *Chem. Rev.* **2012**, *112*, 1001–1033. (e) Ma, L.-Q.; Abney, C.; Lin, W.-B. *Chem. Soc. Rev.* **2009**, *38*, 1248–1256.

(3) (a) O'Keeffe, M.; Yaghi, O. M. *Chem. Rev.* **2012**, *112*, 675–702. (b) Tanaka, D.; Kitagawa, S. *Chem. Mater.* **2008**, *20*, 922–931.

(4) (a) Rowsell, J. L. C.; Yaghi, O. M. *Angew. Chem., Int. Ed.* **2005**, *44*, 4670–4679. (b) Bradshaw, D.; Claridge, J. B.; Cussen, E. J.; Prior, T. J.; Rosseinsky, M. J. *Acc. Chem. Res.* **2005**, *38*, 273–282. (c) Kepert, C. J. *Chem. Commun.* **2006**, 695–700.

(5) Zhang, Z.-J.; Shi, W.; Niu, Z.; Li, H.-H.; Zhao, B.; Cheng, P.; Liao, D.-Z.; Yan, S.-P. *Chem. Commun.* **2011**, *47*, 6425–6427.

(6) (a) Sava, D. F.; Rodriguez, M. A.; Chapman, K. W.; Chupas, P. J.; Greathouse, J. A.; Crozier, P. S.; Nenoff, T. M. *J. Am. Chem. Soc.* **2011**, *133*, 12398–12401. (b) Hasell, T.; Schmidtmann, M.; Cooper, A. I. *J. Am. Chem. Soc.* **2011**, *133*, 14920–14923. (c) Chapman, K. W.; Sava, D. F.; Halder, G. J.; Chupas, P. J.; Nenoff, T. M. *J. Am. Chem. Soc.* **2011**, *133*, 18583–18585. (d) Sava, D. F.; Garino, T. J.; Nenoff, T. M. *Ind. Eng. Chem. Res.* **2012**, *51*, 614–620. (e) Wang, Z.-M.; Zhang, Y.-J.; Liu, T. *Adv. Funct. Mater.* **2007**, *17*, 1523–1536. (f) Dobrzaska, L.; Lloyd, G. O.; Raubenheimer, H. G.; Barbour, L. J. *J. Am. Chem. Soc.* **2006**, *128*, 698–699. (g) Abrahams, B. F.; Moylan, M.; Orchard, S. D.; Robson, R. *Angew. Chem., Int. Ed.* **2003**, *42*, 1848–1851.

(7) Nguyen, S. D.; Yeon, J.; Kim, S.-H.; Halasyamani, P. S. *J. Am. Chem. Soc.* **2011**, *133*, 12422–12425.

(8) Choi, H. J.; Suh, M. P. *J. Am. Chem. Soc.* **2004**, *126*, 15844–15851.

(9) (a) Hertzsch, T.; Budde, F.; Weber, E.; Hulliger, J. *Angew. Chem., Int. Ed.* **2002**, *41*, 2282–2284. (b) Kobayashi, Y.; Jacobs, B.; Allendorf, M. D.; Long, J. R. *Chem. Mater.* **2010**, *22*, 4120–4122.

(10) Zeng, M.-H.; Wang, Q.-X.; Tan, Y.-X.; Hu, S.; Zhao, H.-X.; Long, L.-S.; Kurmoo, M. *J. Am. Chem. Soc.* **2010**, *132*, 2561−2563.
(11) Svensson, P. H.; Kloo, L. *Chem. Rev.* **2003**, *103*, 1650−1681.
(12) Ramette, R. W.; S., R. W. Jr. *J. Am. Chem. Soc.* **1965**, *87*, 5001−5005.
(13) Lu, J. Y. *Coord. Chem. Rev.* **2003**, *246*, 327−347.
(14) Sheldrick, G. M. *SADABS 2.05*; University of Göttingen: Göttingen, Germany, 2002.
(15) *SHELXTL 6.10*; Bruker Analytical Instrumentation: Madison, WI, 2000.
(16) (a) Batten, S. R.; Robson, R. *Angew. Chem., Int. Ed.* **1998**, *37*, 1460−1494. (b) Batten, S. R. *CrystEngComm* **2001**, *18*, 1−7.
(17) Zeng, M.-H.; Zhang, W.-X.; Sun, X.-Z.; Chen, X.-M. *Angew. Chem., Int. Ed.* **2005**, *44*, 3079−3081.
(18) Horike, S.; Tanaka, D.; Nakagawa, K.; Kitagawa, S. *Chem. Commun.* **2007**, 3395−3397.
(19) (a) Zeng, M.-H.; Hu, S.; Chen, Q.; Xie, G.; Shuai, Q.; Gao, S.-L.; Tang, L.-Y. *Inorg. Chem.* **2009**, *48*, 7070−7079. (b) Zhou, Y.-L.; Wu, M.-C.; Zeng, M.-H.; Liang, H. *Inorg. Chem.* **2009**, *48*, 10146−10150. (c) Zeng, M.-H.; Zhou, Y.-L.; Wu, M.-C.; Sun, H.-L.; Du, M. *Inorg. Chem.* **2010**, *49*, 6436−6442. (d) Zeng, M.-H.; Wang, B.; Wang, X.-Y.; Zhang, W.-X.; Chen, X.-M.; Gao, S. *Inorg. Chem.* **2006**, *45*, 7069−7076.
(20) (a) Wang, X.-L.; Qin, C.; Wang, E.-B.; Xu, L. *Eur. J. Inorg. Chem.* **2005**, 3418−3421. (b) Nakagawa, K.; Tanaka, D.; Horike, S.; Shimomura, S.; Higuchi, M.; Kitagawa, S. *Chem. Commun.* **2010**, *46*, 4258−4260.
(21) (a) Kurmoo, M.; Estournes, C.; Oka, Y.; Kumagai, H.; Inoue, K. *Inorg. Chem.* **2005**, *44*, 217−224. (b) Zhang, Z.-H.; Chen, S.-C.; Mi, J.-L.; He, M.-Y.; Chen, Q.; Du, M. *Chem. Commun.* **2010**, *46*, 8427−8429.
(22) Spek, A. L. *J. Appl. Crystallogr.* **2003**, *36*, 7−13.
(23) Privalov, T.; Boschloo, G.; Hagfeldt, A.; Svensson, P. H.; Kloo, L. *J. Phys. Chem. C* **2009**, *113*, 783−790.
(24) (a) Sudik, A. C.; Côté, A. P.; Wong-Foy, A. G.; O'Keeffe, M.; Yaghi, O. M. *Angew. Chem., Int. Ed.* **2006**, *45*, 2528−2533. (b) Newton, G. N.; Cooper, G. J. T.; Kögerler, P.; Long, D.-L.; Cronin, L. *J. Am. Chem. Soc.* **2008**, *130*, 790−791.
(25) Lu, T.-B.; Luck, R. L. *Inorg. Chim. Acta* **2003**, *351*, 345−355.
(26) Volkringer, C.; Loiseau, T.; Guillou, N.; Férey, G.; Elkaïmc, E.; Vimont, A. *Dalton Trans.* **2009**, 2241−2249.
(27) Nakamoto, K. *Infrared and Raman Spectra of Inorganic and Coordination Compounds*; John Wiley and Sons: New York, 2009; pp 1−222.
(28) Zhang, J.-P.; Chen, X.-M. *J. Am. Chem. Soc.* **2008**, *130*, 6010−6017.
(29) (a) Kawano, M.; Fujita, M. *Chem. Soc. Rev.* **2007**, *251*, 2592−2605. (b) Chen, Q.; Zeng, M.-H.; Wei, L.-Q.; Kurmoo, M. *Chem. Mater.* **2010**, *22*, 4328−4334.
(30) Zou, Y.; Hong, S.; Park, M.; Chun, H.; Lah, M. S. *Chem. Commun.* **2007**, 5182−5184.
(31) Bukowska-Strzyzewska, M.; Tosik, A. *Acta Crystallogr., Sect. B* **1982**, *38*, 950−951.
(32) Kurtz, S. K.; Perry, T. T. *J. Appl. Phys.* **1968**, *39*, 3798−3792.
(33) (a) Evans, O. R.; Lin, W.-B. *Chem. Mater.* **2001**, *13*, 2705−2712. (b) Hu, S.; Zou, H.-H.; Zeng, M.-H.; Wang, Q.-X.; Liang, H. *Cryst. Growth Des.* **2008**, *8*, 2346−2351. (c) Wang, Y.-T.; Fan, H.-H.; Wang, H.-Z.; Chen, X.-M. *Inorg. Chem.* **2005**, *44*, 4148−4149.